ELSEVIER

Journal of Molecular Catalysis A: Chemical 167 (2001) 165–170

JOURNAL OF MOLECULAR CATALYSIS A: CHEMICAL

www.elsevier.com/locate/molcata

Computer simulation of surface-point defects interaction in hcp metals

M.I. Pascuet [a], R.C. Pasianot [a,b], A.M. Monti [a,*]

[a] *Depto. Materiales, CNEA, Avda. del Libertador 8250, 1429 Buenos Aires, Argentina*
[b] *CONICET, Buenos Aires, Argentina*

Received 11 April 2000

Abstract

The static relaxation technique is used to analyze the structure of α-Zr and α-Ti perfect surfaces with different orientations as well as their interaction with vacancies and homologous adatoms. Atomic interactions are modeled by many-body potentials of the embedded atom type. Energies and (vibrational) entropies of formation and migration are obtained by minimizing the crystal energy and by further diagonalization of the force constant matrices, respectively. Entropies are calculated at the high temperature limit, considering the atoms as independent oscillators. The more costly coupled oscillators approach is also employed in order to assess the stability of some defect configurations and to envisage reaction coordinates. Relevant results are the following: (a) a lower surface density implies lower formation energies for adatoms and vacancies, but at the same time higher adatom migration energies; (b) surfaces act as sinks, absorbing vacancies and requiring high energies for their reemission; (c) vacancies compete with adatoms as surface diffusion mechanism, the corresponding activation energies being smaller than those for self-diffusion along symmetric grain boundaries and both in turn, smaller than those required for bulk diffusion. © 2001 Published by Elsevier Science B.V.

Keywords: Free surfaces; Diffusion; Point defect properties; Atomistic simulations; hcp Lattices

1. Introduction

It is well known that surfaces play a key role in many material processes such as friction, wear, crack formation, etc. In the last two decades, there has been considerable progress in the study of surface properties from both experimental [1,2] and theoretical points of view [3–6], and computer simulation has proved to be very useful for systems of low symmetry, where analytical calculations are rather difficult. Most studies concentrate on cubic structures, and only perfect surfaces have been investigated in the few dedicated to hexagonal closed packed (hcp) structures [7,8], in spite of the technological relevance of materials such as Zr (nuclear industry) and Ti (aerospace industry).

In this work, we analyze the microstructure of different free surface endings in hcp lattices of α-Zr and α-Ti and their interaction with vacancies and homologous adatoms. We employ the molecular statics method, based on the conjugate gradient technique [9], to perform calculations at 0 K and interatomic potentials of the embedded atom method type (EAM). Formation and migration energies and entropies of vacancies and adatoms are calculated on the relaxed structures, and the results are systematized in terms of the surface density. The paper is organized as follows: in Section 2 we describe the calculation procedure quoting the necessary formulas and concepts, results

* Corresponding author. Fax: +54-11-47547303.
E-mail address: monti@cnea.gov.ar (A.M. Monti).

1381-1169/01/$ – see front matter © 2001 Published by Elsevier Science B.V.
PII: S1381-1169(00)00503-3

are then presented in Section 3 and the conclusions are finally summarized in Section 4.

2. Calculation procedure

According to the EAM scheme, the energy per atom is given by a sum of a pair term and a local volume or density term [10,11]. The interatomic potentials for α-Zr and α-Ti used here are given in references [12,13], respectively; we note that these exactly fit the two lattice parameters *a* and *c*, the five elastic constants, the cohesive energy, and an unrelaxed value of the (bulk) vacancy formation energy, the latter being slightly larger than the experimental value. The hcp structure of both substrata is predicted to be stable with respect to cubic structures and to posses a positive I_2 stacking fault energy. Basic properties of point defects and small vacancy clusters in the bulk [12,13], as well as the structure of symmetric grain boundaries and the interaction vacancy-grain boundary [14], have been previously studied using the same potentials obtaining qualitatively correct results.

The static relaxation technique is used to determine the surface structure by minimizing the crystal energy with respect to the atomic coordinates. A computational supercell with more than 20 relaxable atomic planes parallel to the surface is used, with fixed atomic coordinates for the bottom layers and cyclic boundary conditions on the surface plane. Periodic distances suffice for perfect surface calculations. However, the simulation of point defects on the surface requires of a much larger supercell in order to avoid image interactions.

The surfaces analyzed here are $(0\,0\,0\,1)$, $(1\,0\,\bar{1}\,0)_{\mathrm{C}}$, $(1\,\bar{2}\,1\,0)$ and $(1\,0\,\bar{1}\,0)_{\mathrm{S}}$, ordered according to decreasing atomic density ρ. It has to be noted that in the stacking sequence of the $(1\,0\,\bar{1}\,0)$ planes, CSCSC…, the distance SC doubles the distance CS, and therefore, two surfaces endings are possible [7].

The surface energy E_{S} and surface tension γ are obtained as

$$E_{\mathrm{S}} = \frac{1}{A}\sum_i (E_i + E_{\mathrm{C}}) \quad \gamma = -\frac{1}{4A}\sum_\alpha \left(\sum_{i\neq j} F_{ij}^{\alpha} r_{ij}^{\alpha}\right) \tag{1}$$

where, A the free surface area of the supercell, E_i the energy of the ith atom, E_{C} is the cohesive energy, F_{ij}^{α} is the α-component of the force on the ith atom due to the jth atom and r stands for atomic coordinates. In the formulas above, i runs over all atoms in the supercell, j runs over all their neighbors and α corresponds to two orthogonal directions on the surface. Notice that, E_i converges to $-E_{\mathrm{C}}$ for atoms far enough from the surface.

A vacancy is created in the nth layer away from the very surface by removing an atom, its formation energy $E_{\mathrm{f}}^{\mathrm{vac}}(n)$ is calculated as

$$E_{\mathrm{f}}^{\mathrm{vac}}(n) = E_{\mathrm{rel}}^{\mathrm{vac}}(n) - (E_{\mathrm{rel}} - E_{\mathrm{C}}) \tag{2}$$

where $E_{\mathrm{rel}}^{\mathrm{vac}}(n)$ and E_{rel} are the energies of the relaxed lattices with and without a vacancy, respectively, and E_{C} compensates for the missing atom. This procedure allows us to follow the changes in the vacancy formation energy from the surface into the bulk. A similar expression to Eq. (2) is used for the adatom formation energy, this time inserting an atom on the surface so that $n = 1$ and substituting $+E_{\mathrm{C}}$ for $-E_{\mathrm{C}}$.

Adatoms are only considered to migrate on the top layer, whereas, for vacancies an extended surface region is allowed for and the computations are carried out until bulk values are recovered. The energy for an adatom or vacancy migrating from site (configuration) i to site j, $E_{\mathrm{m}}(i, j)$, is obtained as

$$E_{\mathrm{m}}(i, j) = E_{\mathrm{sad}}(i, j) - E_{\mathrm{eq}}(i) \tag{3}$$

where $E_{\mathrm{sad}}(i, j)$ and $E_{\mathrm{eq}}(i)$ stand for the system energies with the defect in the saddle point potential energy configuration (activated state) and at equilibrium, respectively; also it is true that $E_{\mathrm{sad}}(i, j) = E_{\mathrm{sad}}(j, i)$. The saddle point configuration is obtained by minimizing the energy in the hyperplane of dimension $3N-1$ perpendicular to the reaction coordinate [15,16].

For the purpose of vibrational entropy (S) calculations, the lattice is considered as an assembly of independent (Einstein approximation) or coupled oscillators [17]. The frequencies are the eigenvalues of the coupling matrix ϕ, calculated for EAM potentials according to the expressions given in [11]. The vibrational entropy is generally obtained in the classical high temperature approximation as

$$S = \lim_{N\to\infty} k_{\mathrm{B}} \ln\left(\frac{\prod_{i=1}^{3N}\omega_i^0}{\prod_{i=1}^{3N}\omega_i^{\mathrm{d}}}\right) \tag{4}$$

Table 1
Calculated surface energy E_S and surface tension γ (ergs/cm^2)

		(0 0 0 1)	$(1\,0\,\bar{1}\,0)_C$	$(1\,\bar{2}\,1\,0)$	$(1\,0\,\bar{1}\,0)_S$
Zr	E_S	1070	1147	1264	1437
	γ	1192	590	1211	1868
Ti	E_S	988	1049	1132	1278
	γ	583	369	919	1209

where $\omega_i^0(\omega_i^d)$ is the vibrational frequency of the ith mode of a reference (defective) crystallite containing N atoms, and k_B is the Boltzmann constant. In all entropy calculations for adatoms and vacancies we have employed the Einstein approximation, taking the relaxed configuration of the free surface as the reference lattice, and replacing the limit $N \to \infty$ in Eq. (4) by the contributions of all the atoms in the (periodic) supercell [18].

3. Results

In Table 1, we report the surface energy E_S and surface tension γ calculated according to Eq. (1) for the four surfaces considered after lattice relaxation. Experimental values of γ, taken on policrystals and extrapolated to 0 K [19] are 2734 ergs/cm^2 for Zr and 2881 ergs/cm^2 for Ti. Note that, there is an inverse correlation between E_S and the surface density ρ. A similar correlation seems to be valid for γ, the more compact surfaces endings (0 0 0 1) and $(1\,0\,\bar{1}\,0)_C$ being, however, interchanged. These tendencies agree with previous calculations by Fernández [20] using other EAM potentials.

Table 2 shows the computed formation energies E_f for adatoms and vacancies in the top layer. Both metals and type of defects show that a lower surface density implies lower formation energy. The slightly negative/positive values for adatoms/vacancies on the $(1\,0\,\bar{1}\,0)_S$ surface indicate a trend in favor of ending C, less energetic than ending S. Bulk (calculated) values of E_f for vacancies are 1.74 for Zr and 1.51 eV for Ti, considerably larger than the reported figures in Table 2, but generally recovered starting from the fourth layer. We note that with the exception of surface (0 0 0 1) the vacancy is predicted unstable in some layers near the surface, namely: the third one of ending $(1\,0\,\bar{1}\,0)_C$, and the second and third ones of endings $(1\,\bar{2}\,1\,0)$ and $(1\,0\,\bar{1}\,0)_S$. Such instabilities are observed in some cases during the energy minimization process, vacancies evolving spontaneously towards the top layer. In other cases, although vacancies remain at their original positions, an analysis of vibrational modes for clusters of around 150 coupled atoms reveals instabilities through either imaginary or very small, but real frequencies.

Table 2
Formation energies E_f of adatoms and vacancies on the top layers of different Zr and Ti surfaces (eV)

		(0 0 0 1)	$(1\,0\,\bar{1}\,0)_C$	$(1\,\bar{2}\,1\,0)$	$(1\,0\,\bar{1}\,0)_S$
Zr	Adatom	1.11	0.64	0.39	≤ -0.01
	Vacancy	0.87	0.46	0.41	0.09
Ti	Adatom	1.08	0.62	0.33	−0.04
	Vacancy	0.85	0.44	0.34	0.04

Fig. 1 shows the lowest energy migration jumps for the adatoms on the four surfaces studied. Our potentials predict slightly different equilibrium positions for the adatom in Zr and Ti; as a consequence, long range migration requires two different jumps in Zr, but only one in Ti for the (0 0 0 1) and$(1\,0\,\bar{1}\,0)_C$ surfaces. The corresponding numerical values of migration energies E_m are quoted in Table 3. E_m values are predicted to increase with surface roughness. Also, migration is found two-dimensional and isotropic on the (0 0 0 1) surface and practically one-dimensional on the others, confined to a zigzag channel parallel to the c-axis for the $(1\,\bar{2}\,1\,0)$ surface and to the direction perpendicular to the c-axis for the $(1\,0\,\bar{1}\,0)$ surfaces.

Regarding the vacancy migration, we collect in Table 4 the results obtained for the jumps in the surface layer and from and to the surface layer. All jumps reported are between first neighbors (in or out of plane). For bulk migration, the predicted values are 0.58 eV for Zr and 0.50 eV for Ti. The results indicate the character of vacancy sink exhibited by the surfaces, thus requiring high energies for emission and very low ones for absorption.

Adatom and vacancy formation entropies S_f calculated for the top layer according to the Einstein approximation, are reported in Table 5. Although S_f decreases with the surface density in Zr for both point defects, no such a correlation can be established in Ti. However, it is still predicted that on the more compact

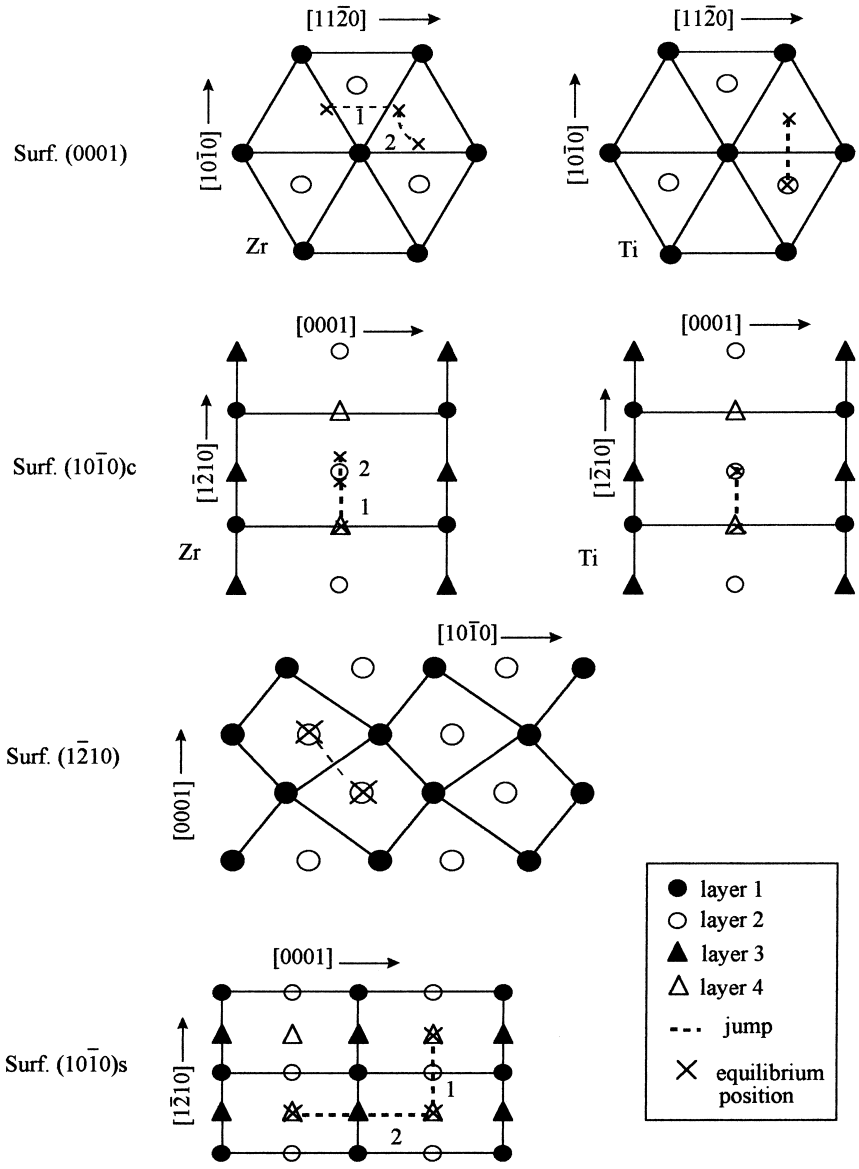

Fig. 1. The lowest energy migration jumps for the adatom on the four surfaces studied, numbers 1 and 2 indicate different jumps.

surfaces the entropy for adatoms is higher than for vacancies. In addition, the values for vacancies on the different surfaces are significantly lower than the corresponding bulk values. These are, in units of k_B: 4.15 and 4.08 for Zr, and 1.39 and 2.05 for Ti [14]. The first value of each pair corresponds to a calculation under constant volume and the second one is for constant pressure. In this sense, note that calculations for the vacancy on the surface are carried out under mixed conditions.

For comparison purposes we calculate the formation free energy $G_f = E_f - TS_f$. According to Tables 2 and 5, in all surfaces except $(1\,0\,\bar{1}\,0)_S$, G_f is mainly contributed by the formation energy term. The rela-

Table 3
Adatom migration energies E_m (eV)[a]

	(0 0 0 1)	$(1\,0\,\bar{1}\,0)_C$	$(1\,\bar{2}\,1\,0)$	$(1\,0\,\bar{1}\,0)_S$
Zr	0.02 (1)	0.07 (1)	0.19	0.35 (1)
	∼0 (2)	∼0 (2)		1.62 (2)
Ti	0.063	0.083	0.21	0.38 (1)
				0.72 (2)

[a] (1) and (2) refer to the jumps indicated in Fig. 1.

Table 4
Vacancy migration energies E_m (eV)[a]

	Jumps	(0 0 0 1)	$(1\,0\,\bar{1}\,0)_C$	$(1\,\bar{2}\,1\,0)$	$(1\,0\,\bar{1}\,0)_S$
Zr	1 → 1	0.44	0.58	0.35	0.38
	1 → 2	1.02	0.88	≥1.10	0.74
	2 → 1	0.09	0.10	–	–
Ti	1 → 1	0.45	0.60	0.35	0.40
	1 → 2	0.84	0.82	0.73	0.71
	2 → 1	0.06	0.08	–	–

[a] 1 → 1 indicates jumps within the same surface layer, 1 → 2 jumps from the surface layer to the layer below, and 2 → 1 the converse ones. Missing values correspond to the vacancy instability in the second layer.

tion TS_f/E_f, evaluated at 300 K, amounts to no more than 10% for all surfaces except for the $(1\,0\,\bar{1}\,0)_S$ where it may be up to 100%. This is a consequence of the extremely low formation energy values for this surface.

The defect equilibrium concentration, as obtained from standard thermodynamics [21], is given by $C_{eq} = \exp(-G/k_BT)$. In Table 6, we report the equilibrium concentrations calculated at 300 K for each defect type and surface orientation. The abnormally high concentration predicted for the $(1\,0\,\bar{1}\,0)_S$ surface can be understood as a consequence of the previously

Table 5
Adatom and vacancy formation entropies S_f (in units of k_B)

		(0 0 0 1)	$(1\,0\,\bar{1}\,0)_C$	$(1\,\bar{2}\,1\,0)$	$(1\,0\,\bar{1}\,0)_S$
Zr	Adatom	4.68	2.18	0.48	0.41
	Vacancy	2.55	1.50	0.77	0.69
Ti	Adatom	2.15	1.35	0.57	0.83
	Vacancy	0.89	0.63	0.90	−0.11

Table 6
Defect equilibrium concentration at 300 K

		(0 0 0 1)	$(1\,0\,\bar{1}\,0)_C$	$(1\,\bar{2}\,1\,0)$	$(1\,0\,\bar{1}\,0)_S$
Zr	Adatom	$2.3\ 10^{-17}$	$1.5\ 10^{-10}$	$4.5\ 10^{-7}$	∼1
	Vacancy	$3.0\ 10^{-14}$	$8.3\ 10^{-8}$	$2.8\ 10^{-7}$	$6.0\ 10^{-2}$
Ti	Adatom	$6.0\ 10^{-18}$	$1.4\ 10^{-10}$	$5.0\ 10^{-6}$	>1
	Vacancy	$1.2\ 10^{-14}$	$7.5\ 10^{-8}$	$4.7\ 10^{-6}$	$1.9\ 10^{-1}$

Table 7
Activation energy Q (eV)

		(0 0 0 1)	$(1\,0\,\bar{1}\,0)_C$	$(1\,\bar{2}\,1\,0)$	$(1\,0\,\bar{1}\,0)_S$
Zr	Adatom	1.10	0.71	0.58	∼0.35
	Vacancy	1.31	1.04	0.76	0.47
Ti	Adatom	1.14	0.70	0.54	∼0.38
	Vacancy	1.30	1.04	0.69	0.44

mentioned tendency of this surface to evolve towards the $(1\,0\,\bar{1}\,0)_C$ one by defect generation. Table 6 also indicates that vacancies are predominant on the two more compact surfaces, but adatoms compete on the $(1\,\bar{2}\,1\,0)$ one.

Finally, in Table 7 we collect the results for the diffusion activation energy on the different surfaces $Q = E_f + E_m$. It is worthwhile to note the similarity in the values of Q predicted on both materials for each defect type.

4. Conclusions

We have presented a rather comprehensive computer simulation study of the statics and the dynamics of vacancies and adatoms on different surface orientations in two hcp materials.

A characterization of the free surfaces indicates an inverse correlation between surface density and surface energy, the same seems to hold for the surface tension if (0 0 0 1) and $(1\,0\,\bar{1}\,0)_C$ are interchanged in the sequence. Contrary, the adatom and vacancy formation energies increase with the surface density. Neglecting relaxation contributions, the above findings for energies are expected from a simple broken/restituted bonds analysis. Room temperature defect concentrations follow the trend imposed by the

formation energies due to the negligible entropy contribution. The abnormally high values predicted for the $(1\,0\,\bar{1}\,0)_S$ surface area consequence of this surface's tendency to evolve towards the $(1\,0\,\bar{1}\,0)_C$ one by defect generation.

A large decrease of the vacancy formation energy on the surface top layer with respect to the bulk value is obtained. This result was previously reported by Wynblatt and Gjostein [22] in different Cu surfaces modeled by pair potentials and by Karimi et al. [5] for Pb(1 1 0) with EAM potentials. The present results indicate that bulk values are generally recovered starting from the fourth layer. The formation entropy shows a similar behavior for the most compact endings (0 0 0 1), $(1\,0\,\bar{1}\,0)_C$, however, the bulk value is not obtained until the eighth layer for $(1\,\bar{2}\,1\,0)$ while it still remains 10% below for $(1\,0\,\bar{1}\,0)_S$. This implies that the "surface" comprises a small region extending about 15 Å.

Calculations of vacancy migration energy from/to the bulk indicate the character of vacancy sink exhibited by the surfaces. For adatoms, migration turns out to be more difficult with surface roughness; it is two-dimensional and isotropic on the (0 0 0 1) surface and practically one-dimensional on the others, imposed by the surface symmetries. Its is worth to note that, our results do not explicitly include thermal effects, that may somewhat change this picture [4].

The comparison among the activation energy values for bulk Q_b, symmetric grain boundaries Q_{gb} [14] and the present for surfaces Q, obtained by the same simulation technique and interatomic potentials here used, shows the pattern $Q < Q_{gb} < Q_b$ as is generally expected [21,23]. However, a more complete description of surface diffusion requires considering correlation effects, which may be particularly important in the presence of anisotropic migration [24], such as that referred to above.

Acknowledgements

This work was partially supported by CONICET through PIP 4205/1295.

References

[1] D.J. Trevor, Ch.E.D. Chidsey, D.N. Loiacono, Phys. Rev. Lett. 62 (1989) 929.
[2] J.K. Gimzewski, R. Berndt, R.R. Schlittler, Phys. Rev. B 45 (1992) 6844.
[3] J.C. Tully, G.H. Gilmer, M. Shugard, J. Chem. Phys. 71 (1979) 1630.
[4] G. De Lorenzi, G. Jacucci, V. Pontikis, Surf. Sci. 116 (1982) 391.
[5] M. Karimi, G. Vidali, I. Dalins, Phys. Rev. B 48 (1993) 8986.
[6] I. Vattulainen, J. Merikoski, T. Ala Nissila, S.C. Ying, Phys. Rev. B 57 (1998) 1896.
[7] S.P. Chen, Surf. Sci. 264 (1992) L162.
[8] J.R. Fernandez, A.M. Monti, R.C. Pasianot, Philos. Mag. B 75 (1997) 283.
[9] R. Fletcher, C.M. Reeves, Comput. J. 7 (1964) 149.
[10] M.S. Daw, M.I. Basques, Phys. Rev. B 29 (1984) 6443.
[11] M.W. Finnis, J.E. Sinclair, Philos. Mag. A 50 (1984) 45.
[12] R.C. Pasianot, A.M. Monti, J. Nucl. Mater. 264 (1999) 198.
[13] J.R. Fernández, A.M. Monti, R.C. Pasianot, J. Nucl. Mater. 229 (1995) 1.
[14] J.R. Fernandez, A.M. Monti, R.C. Pasianot, V. Vitek, Philos. Mag. 80 (2000) 1349.
[15] G.H. Vineyard, J. Phys. Chem. Solids 3 (1957) 121.
[16] A.M. Monti, E.J. Savino, Phys. Rev. B 23 (1981) 6494.
[17] R.D. Hatcher, R. Zeller, P.H. Dederichs, Phys. Rev. B 19 (1979) 5083.
[18] J.R. Fernández, A.M. Monti, R.C. Pasianot, Phys. Stat. Sol. 219 (2000) 245.
[19] L.E. Murr, Interfacial Phenomena in Metals and Alloys, Addison-Wesley, Reading, MA, 1975.
[20] J.R. Fernandez, Ph.D. Thesis, Univ. de Córdoba, Argentina, 1994.
[21] N.A. Gjostein, Diffusion, American Society of Metals, Cleveland, OH, 1973.
[22] P. Wynblatt, N.A. Gjostein, Surf. Sci. 12 (1968) 109.
[23] Y. Adda, J. Philibert, La Diffusion dans les Solides, Tome II, Presses Universitaires de France, France, 1966.
[24] Y.M. Mishin, Ch. Herzig, Philos. Mag. A 71 (1995) 641.